

Open low speed wind tunnel – design and testing

RYSZARD SZWABA
KRZYSZTOF HINC
TOMASZ OCHRYMIUK
ZBIGNIEW KRZEMIANOWSKI
PIOTR DOERFFER
MARCIN KUROWSKI*

Institute of Fluid Flow Machinery, Polish Academy of Sciences,
Fiszera 14, 80-231 Gdansk, Poland

Abstract This paper presents the design method and the construction details of a subsonic low-speed wind tunnel, which has been designed to achieve the flow velocity of 35 m/s in the measurement section with expected uniform velocity field at its inlet. To achieve such objectives a very detailed design was performed using a theoretical 1D analysis and computational fluid dynamics simulations. This approach was applied to improve the flow quality along the wind tunnel sections. When the wind tunnel has been launched a direct comparison of the experimentally measured flow field in the test section and numerical simulation results was conducted. Such comparison of the simulation results with the experimental one is presented in this paper. The obtained results confirm that assumed wind tunnel design method was correct, *i.e.* the pressure drop in the wind tunnel has been predicted very well and drive system is effective and sufficient to accelerate the airflow to required values.

Keywords: Wind tunnel; Wind tunnel design; Wind tunnel measurements

1 Introduction

The low-speed experimental aerodynamics since it was established in previous century continues its evolution and features an important role in the development of a wide range of devices that must perform their functions

*Corresponding Author. Email: marcin.kurowski@imp.gda.pl

in the face of forces imposed by strong flows of air. Despite the quick and intensive development of computational fluid dynamics (CFD) and its more attractive option to obtain results for many engineering applications, better in cost-effectiveness, the simulations have not approached a sufficient level to replace experiments [1–3]. Therefore, the use of wind tunnels, especially in the subsonic regime is necessary for validation of newly designed machines and devices exposed to aerodynamic loads. Aerodynamic tunnels are designed for specific types of applications and one cannot say about some universal aerodynamic tunnel. Similar approach has been applied for the tunnel design presented in this paper. It has been mainly intended for testing the characteristics and loads of wind turbine models used in the urbanized area, as well as for small models of all types of road and flying vehicles.

This paper describes the design method and the construction details of a medium size subsonic low-speed wind tunnel, which has been designed to achieve the flow velocity up to 35 m/s in the working section with expected uniform velocity field at its inlet, making it available for research of low speed wind turbines aerodynamics, flight and traffic vehicles, sport activities, civil engineering applications, fundamental research in fluid mechanics [4, 5] and other possibilities. To achieve such objectives a very detailed design was performed using theoretical 1D analyses and CFD simulations. This approach was applied to improve the flow quality along the wind tunnel sections. Design of the inlet, fans setting and the electrical engines assembly inserted in a ‘suction’ configuration required a lot of attention. Appropriate screens and honeycombs are applied at the inlet section for control and stabilization of the flow to induce the low drag level in the test section. The design and construction of each wind tunnel section have been presented and discussed focusing on the most relevant technical aspects. Some design and manufacture guidance for the main components of a subsonic wind tunnel is also presented.

2 Wind tunnel design

Several references [6–10] for wind tunnel design can be found in the literature. However, to ensure the uniformity of the flow inside the designed wind tunnel as well as the cost requirements and manufacturing process required a lot of attention and effort. According to these references, some rules can be applied with small corrections or adjustments for each specific design and application.

The main requirements for the specifications of wind tunnel were defined at the beginning as: low-speed (at subsonic Mach number, $M = 0.1$) wind tunnel for research and commercial purposes, open-circuit/closed test section with inlet stabilization section. The open circuit type results from the limited space available in the laboratory building. For such construction one can obtain relatively large cross-section of testing part in relation to the wind tunnel length. The design criteria have been set to enable accurate measurements of steady or unsteady flow with low drag to facilitate low cost of operation and of course the study of the physical phenomena of interest. Additionally, also other requirements were considered in the wind tunnel design, *i.e.* for accurate flow field and aeroacoustics analysis. According to these requirements, the main characteristics of the wind tunnel were defined as:

- Open-circuit wind tunnel of approximately 15 m in length and 6 m in height.
- A test space with the cross-section of order $2 \text{ m} \times 2 \text{ m}$ and length of 4 m.
- The maximum air velocity at the test chamber must reach 35 m/s ($M \approx 0.1$).
- Minimum flow velocity: 3 m/s.
- Inlet size appropriate to test section dimensions.
- Inclusion of an inlet stabilization zone with honeycomb for passive flow control.
- Outlet diffuser divided into 16 sections.
- The wind tunnel material should be plywood plates for covering the sides of sections. Requirements for surface have been considered to be waterproof and low roughness. The major structure (skeleton) should be metal elements.
- Drive system: 16 electrical engines, three-phase of 400 V and power adequate to total tunnel drag at maximal velocity.
- Engine speed control: through frequency inverter.
- Fan blades with geometry that ensure the required pressure drop and for reaching optimum operational condition.
- The drive system must be structural isolated from other sections of the tunnel to avoid vibration.

The first stage of the design process was a determination of major dimensions of the wind tunnel according to the assumptions. Next, the analytical 1D approach was used to estimate the pressure drop at operational design points to determine the tunnel working parameters and enable the selection of an appropriate drive system.

A separate task was to design the shape of the tunnel inlet in a way to ensure along the limited space uniform, unseparated and undisturbed stream at the inlet of the measurement section. This task was performed by means of CFD simulations. The goal in this case is the dimension of cross-section of the test chamber. The inlet wall shape was preliminary designed based on a typical 1D formula for nozzles design [11] and followed by the CFD calculations. In the next step the inlet wall profile was updated based on the streamlines coming from the far-field flow which took the surrounding into consideration. After few iterations a required shape for inlet of the wind tunnel with uniform and unseparated flow may be received. The shape of an inlet and the example of the result of velocity distribution at the tunnel inlet is shown in Fig. 1. In this case the local velocity is imposed on the surface tunnel wall. This result shows that the flow velocity after acceleration around the inlet mouth gradually decreases until it reaches the desired value and uniform distribution at the outlet, thereby at the test section inlet.

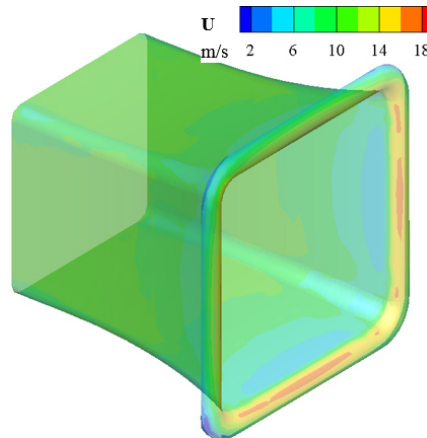


Figure 1: Local velocity distribution at the tunnel inlet.

As it was mentioned before there was a limited space available in the laboratory building and this fact also had an impact on the diffuser construction. The diffuser had to be shorter than it results from condition for

unseparated flow in such devices. To overcome this constraint the whole diffuser was divided into 16 even parts, one can say into 16 small sub-diffusers. Such solution, although increases the tunnel drag, allows to avoid large flow separation in the shorter diffuser. In the end, the diffuser division made that the half angle of its walls deviation not exceeds 5° and additionally such solution together with separate fans for each subdiffuser allow to control the velocity distribution in the cross-section of test chamber. The sketch view of the wind tunnel diffuser is presented in Fig. 2.

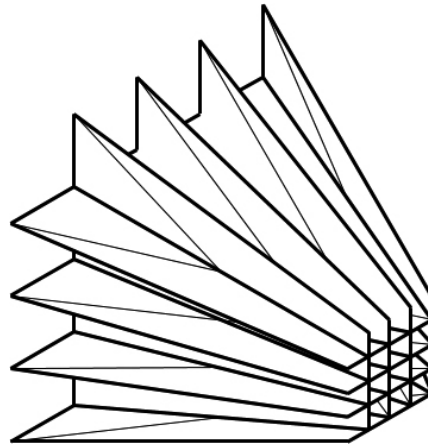


Figure 2: Sketch view of the diffuser.

The assumptions for the design of test chamber were quite simple because it has a constant cross-section with the determined length. Additionally, between the inlet and test section a flow stabilization section with honeycomb is placed. After the preliminary designs of the inlet, stabilization section, measurement section and diffuser a concept of a complete wind tunnel with the drive system could be designed. Figure 3 shows a schematic view of the open-circuit wind tunnel and its particular parts (sections). As one can see the wind tunnel consist of the following elements: streamline shape inlet, stabilization section, measurement section, diffuser and drive system with fans. The air in the tunnel flows from inlet (no. 1) throughout its particular parts to the suction fans section (no. 5), hence the fans are located downstream of the measurement section.

One of the last missing elements to complete the wind tunnel designing is a power of the drive system and compression of the fans. To asses these values the pressure drop in the tunnel should be calculated precisely. Gen-

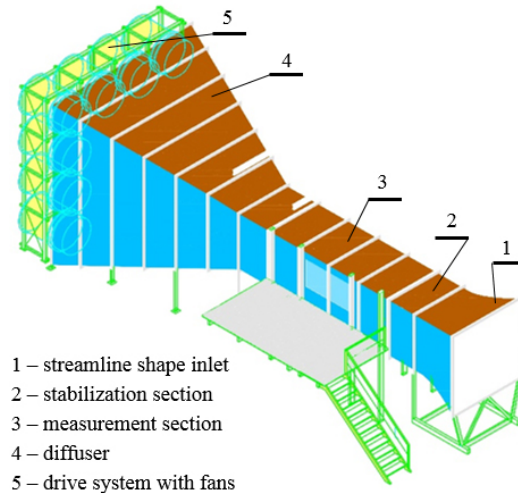


Figure 3: Open-circuit wind tunnel – sketch and description.

erally, pressure losses during the fluid flow through a channel limited by walls are caused by irreversible conversions of mechanical energy into heat. One can distinguish two types of losses in the flow, namely losses related to the existence of the friction phenomenon (*i.e.* boundary layer), and local losses, *i.e.* change in cross-sections, obstacles, etc. The first of these depend on the fluid viscosity that influences its movement in the channel, causing momentum exchange between adjacent layers. The second of these losses occurs as a result of the disturbances existing in the flow caused by the varied so called obstacles, whereby the energy carried by the flow is shed.

2.1 One-dimensional theory – basic calculations

Calculations of the total pressure losses in fluid flow in the wind tunnel with the shape and main dimensions, shown in Fig. 4, were made using the one-dimensional theory (1D) based on the handbook of hydraulic resistance [12]. Basically, one-dimensional theory has been used in technology for a long time and it is based on a solid long-term experimental experience. It should be added that the accuracy of 1D theory depends on the coefficients, which are used for calculation. If the coefficients are correctly defined, this theory is a very useful tool because of its simplicity and swiftness, which can accurately determine the loss of total pressure during the fluid flow through a channel of any shape.

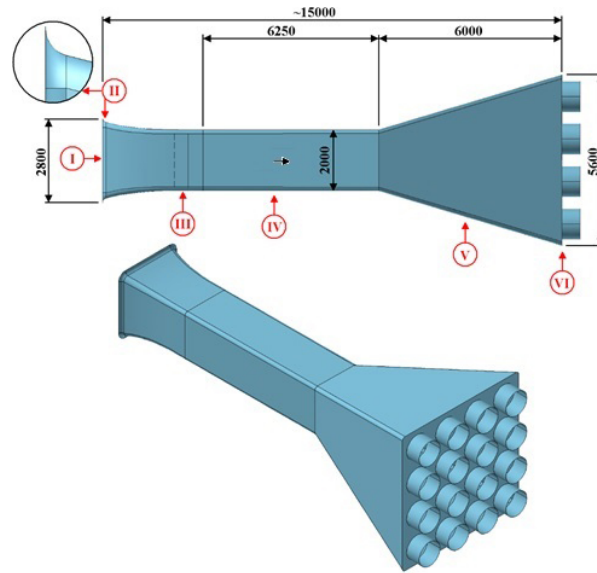


Figure 4: Wind tunnel geometry used in CFD calculation and total pressure losses.

The modelled wind tunnel was made of a waterproof plywood, therefore a relatively low surface roughness of $20 \mu\text{m}$ was assumed. At the inlet of the measurement section a honeycomb of 0.3 m length was used to stabilize and uniform the flow in this location. The main assumption for the calculations was that the air velocity in the measurement part of the tunnel (no. 3 in Fig. 3) should reach the value of 35 m/s . On this basis, the velocity in the other elements of the flow system has been calculated from the mass conservation equation. Density and viscosity of the air were assumed for 293 K . For 1D analysis, the tunnel was divided into six main parts, Fig. 4, namely: I) confusor – inlet, II) rounding radius at inlet, III) honeycomb screen, IV) rectilinear part, V) diffuser, VI) local surface discontinuity, related to the cross-section change between the diffuser and fans. Behind the section VI, there are rectilinear round pipes that simulated the ducts for 16 axial fans (4×4).

The total pressure losses in the tunnel Δp_{tot} for the elements: I) Δp_{con} , II) Δp_{rad} , III) Δp_{scr} , V) Δp_{dif} , and VI) Δp_{ch} were determined using the general following formula: $\zeta \rho U^2 / 2$, where ζ is the factor of local losses, ρ is the density of the fluid and U is the velocity in the cross-section with a smaller area. The total pressure loss in the part of the tunnel with a constant cross section IV) Δp_{lin} was determined using the general formula

with the shape $\zeta\rho(L/D)U^2/2$, where ζ is the coefficient of linear losses, L is the length of this element, while D is its hydraulic diameter. Table 1 summarizes the result of the total pressure drops calculations in individual elements of the wind tunnel.

Table 1: Total pressure losses of the wind tunnel elements.

Tunnel element	Variable	Value (Pa)
Confusor, inlet	Δp_{con}	25
Inlet radius	Δp_{rad}	121
Honeycomb	Δp_{scr}	35
Test section	Δp_{lin}	32
Diffuser	Δp_{dif}	515
Cross-section change	Δp_{ch}	22
Summary	Δp_{out}	749

3 Numerical and experimental setup

After the inlet and other particular parts of the wind tunnel design and drive system selection, the detailed CFD simulations and analysis of whole wind tunnel with 3D geometry have been made. The final corrections based on the CFD results of the wind tunnel geometry were applied and then the tunnel construction was designed and manufactured.

3.1 Numerical model description

The computational analyses were performed to provide a general description and quality of the flow inside the whole wind tunnel. The 3D numerical simulations have been performed by means of the commercial code Ansys/Fluent [13]. The $k-\omega$ shear stress transport (SST) turbulence model was used in the calculations, which was a compromise between the computational resources and satisfactory numerical results. Third order MUSCL (monotonic upstream-centered scheme for conservation laws) scheme was used for spatial discretization. Inlet/outlet boundary conditions are shown in Table 2. Boundary conditions at the outlet were adjusted in order to keep the required velocity in the test section.

Turbulent intensity at given hydraulic diameter was equal to 3% and inlet flow temperature was 20°C for all flow cases. The geometry of the test section including inlet, honeycomb screen, test section, diffuser and

Table 2: Boundary conditions of the 3D calculations.

Section	Parameter	Value	Unit
	Total pressure	101	kPa
Inlet	Total temperature	297	K
	Viscosity ratio	10	–
Outlet	Velocity	3.2 11.0	m/s

fan tubes is shown in Fig. 4. Computational mesh was created using Ansys/Meshing software [14]. Honeycomb screen was modelled using the replacement porous model [15, 16]. The computational domain was an accurate representation of experimental test section plus ambient zone at inlet and the mesh contained about 20 M elements. Unstructured hexahedral mesh was refined close to the wall to keep parameter $y^+ \sim 1$ (dimensionless distance to the wall) in all sections. High refinements level gives sufficient prediction of the developing flow and its pressure losses.

3.2 Experimental setup

One of the main measurement systems of the built wind tunnel is the array of robust ceramic sensors for flow velocity field measurement set in the particular plane. For this purpose the array of nine TSI 8455 probes was mounted on a common aerodynamic profile, see Fig. 5. The distance between the probes is 0.2 m. The aerodynamic bar with velocity measurement probes is connected to automatic transportation system, which facilitates the velocity measurement in the chosen plane along the measurement chamber, Fig. 4 – IV. The measurement accuracy of TSI probes depends on the



Figure 5: Velocity measurement array.

selected range of the velocity transducer and basically equals to $\pm 0.5\%$ of selected range plus 2% of reading. During the wind tunnel commissioning and testing the selected range was 0 – 50 m/s and average velocity in flow field measurement in the test section was 10 m/s, hence all together imply on accuracy of measurement velocity about ± 0.45 m/s. The averaging time of the velocity during the measurement was equal to 10 s.

The measurement of stagnation parameters took place at the inlet of measurement section by the Prandtl probe and K-type thermocouple. The pressure was measured by means of a pressure transducer with ± 1.0 Pa accuracy and the temperature was measured by means of the thermocouple element of ± 0.5 K accuracy.

4 Results and discussion

When the stages of wind tunnel building and commissioning of measurement systems was finished it was possible to compare directly the flow field in the test section measured experimentally with the numerical simulation results. The measurement of velocity field distribution in several subsequent planes in the section is shown in Fig. 6. The coordinate $X = 0$ starts at the inlet to measurement section, *i.e.* on the junction between the element I and IV in Fig. 4. The first plane was measured at $X = 400$ mm, then next at $X = 1000$ mm, and next ones every 500 mm to the last at $X = 4000$ mm.

As one can see in Fig. 6 that velocity distribution in particular plane is quite uniform and in general the values do not exceed ± 0.5 m/s from the average value what is within the measurement accuracy of the used

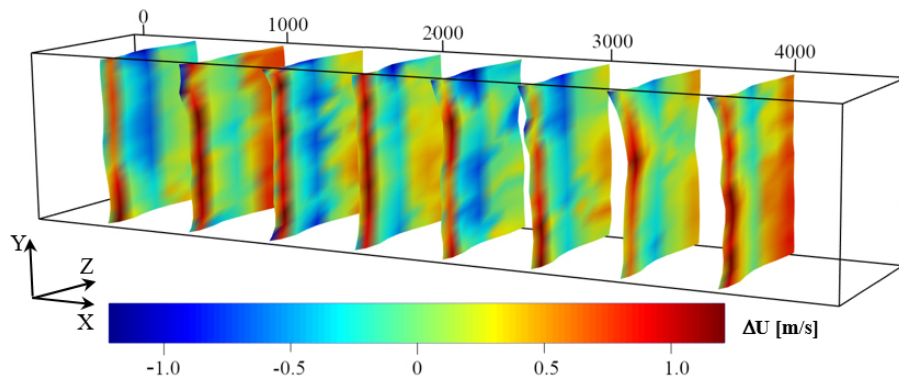


Figure 6: Velocity distribution in several planes in the test section of the wind tunnel.

measuring sensors. The obtained results show that assumption of the design process to have a uniform velocity field in the measurement section has been achieved, hence these results also show that the inlet geometry based on the streamline shape was designed properly.

For the flow case shown above, the numerical simulation was carried out, as well. As the simulation was steady so the obtained flow field is constant in the same planes as in experiment, except the viscous regions near the walls. The comparison of the average velocity obtained from CFD with experimental data for the same area in particular planes is shown in Table 3.

Table 3: Average velocity comparison.

Position X (mm)	CFD mean (m/s)	Measure mean (m/s)
400	10.18	10.54
1000	10.21	10.23
1500	10.23	10.27
2000	10.25	10.58
2500	10.27	10.32
3000	10.29	10.35
3500	10.31	10.46
4000	10.32	10.34

Table 3 shows that in case of CFD one can observe very slow velocity increase along the test section channel coupled to development of wall boundary layer. The experimental results show that the flow velocity in the channel is more or less constant indicating a slight deviation from the mean value, in this case it is 0.15 m/s.

In order to predict the proper flow losses in the wind tunnel it is worth to compare CFD simulation with experimental data. A comparison of the velocity profiles in the boundary layer for CFD and experiment at the beginning of the test section at $X = 400$ mm is shown in Fig. 7. The comparison of integral parameters of these two boundary layers is also presented in Table 4. The boundary layer parameters, such as thickness, δ , displacement and momentum thickness, δ^* and δ^{**} , respectively, were calculated using equations for the boundary layer in a compressible flow. Fig. 7 shows very good agreement of boundary layer profile obtained from CFD with the experimental data, the shape parameters are very similar. The numerical simulation predict higher values of other parameters, *i.e.*

the boundary layer thickness, which is the result of worse fulfilment of the profile in its upper (wake) part.

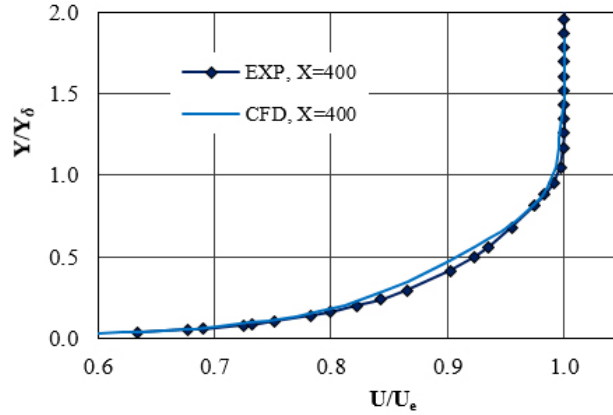


Figure 7: Normalized boundary layer velocity profiles; Y_d – boundary layer thickness, U_e – freestream velocity.

Table 4: Boundary layer integral parameters.

Parameters	Symbol	Unit	Experiment	CFD
Thickness	δ	mm	54	82
Displacement thickness	δ^*	mm	6.9	10.6
Momentum thickness	δ^{**}	mm	4.8	7.2
Shape parameter	$H = \delta^*/\delta^{**}$	–	1.44	1.38

As the design point of the constructed wind tunnel was to achieve the flow velocity up to 35 m/s at the inlet to the measurement section, the appropriate CFD simulation has also been performed. This simulation was carried out to double check the total losses assessment. The numerical simulations for such flow condition give the total losses at the level around 700 Pa. Compared with the 1D method presented in previous section the obtained difference was around 6%, which is a good and acceptable result.

Once the losses in particular parts of the wind tunnel were known and hence in the whole wind tunnel itself one would need to select the basic parameters of the tunnel drive system, *i.e.* an electric engine power and compression of the single fan. Taking into account some safety factor and accessible fans on the market it was decided to assemble in the wind tunnel an array of 16 fans with the power of 20 kW each and 1000 Pa of compres-

sion rate. The first commissioning of the built new wind tunnel shows that velocity of assumed design point was easily achieved, what confirms that the assumptions made during the design of the wind tunnel were proper.

5 Conclusion

The paper describes the design method and the construction details of a medium size, open loop, subsonic low-speed wind tunnel. The presented method is based on a comprehensive analysis by means of theoretical 1D hydraulic resistance theory supported by detailed computational fluid dynamics simulations of the inlet and the whole wind tunnel. This approach was applied to improve the flow quality along the wind tunnel sections, hence the inlet geometry based on the streamline shape was designed properly.

The obtained results confirm that assumed wind tunnel design method was correct, *i.e.*, the pressure drop in the wind tunnel has been predicted very well and drive system is effective and sufficient to accelerate the airflow to required values. The flow field in the test section also fulfils the expected values and quality:

- flow velocity after acceleration around the inlet mouth gradually decreases reaching an uniform distribution at the test section inlet,
- velocity distribution in the measurement section is satisfactory uniform and its deviation from average values comprises within the measurement accuracy.

Received 7 September 2020

References

- [1] BARLOW J.B., RAE JR W.H., POPE A.: *Low-Speed Wind Tunnel Testing*. John Wiley and Sons; New York 1999.
- [2] BRADSHAW P., PANKHURST R.C.: *The design of low-speed wind tunnels*. Prog. Aerosp. Sci. **5**(1964), 1–69.
- [3] ANDERSON J.D. JR.: *Fundamentals of Aerodynamics* (5th Edn.). McGraw-Hill; 2011.
- [4] KNEBA Z.: *Modeling of the internal combustion engine cooling system*. Arch. Thermodyn. **40**(2019), 3, 109–121.

-
- [5] MUSZYŃSKI T., ANDRZEJCZYK R., PARK W.I., DORAO C.A.: *Heat transfer and pressure drop characteristics of the silicone-based plate heat exchanger*. Arch. Thermodyn. **40**(2019), 1, 127–143.
- [6] MEHTA J., BRADSHAW P.: *Design rules for small low speed wind tunnels*. Aeronaut. J. **83**(1979), 827, 443–453.
- [7] STATHOPOULOS T.: *Design and fabrication of a wind tunnel for building aerodynamics*. J. Wind Eng. Ind Aerod. **16**(1984), 2–3, 361–376.
- [8] CATTAFESTA L., BAHR C., MATHEW J.: *Fundamentals of wind-tunnel design*. In: *Encyclopedia of Aerospace Engineering*. John Wiley and Sons, Hoboken 2010.
- [9] BELL J.H., MEHTA R.D.: *Boundary-layer predictions for small low-speed contractions*. AIAA J. **27**(1989), 3, 372–374.
- [10] NOOR A., ED.: *Wind Tunnel Designs and their Diverse Engineering Applications*. IntechOpen, 2013.
- [11] DISCETTI S., IANIRO A., AREF H.: *Experimental Aerodynamics*. CRC Press – Taylor & Francis Group; Boca Raton 2017.
- [12] IDELCHIK I.E.: *Handbook of Hydraulic Resistance. Coefficients of Local Resistance and of Friction*. US Atomic Energy Commission and the National Science Foundation. Washington DC 1966.
- [13] Ansys Fluent Fluid Simulation Software <https://www.ansys.com/products/fluids/ansys-fluent> (access: 5 Jan. 2020).
- [14] Ansys Meshing <https://www.ansys.com/products/platform/ansys-meshing> (access: 5 Jan. 2020).
- [15] OCHRYMIUK T.: *Numerical analysis of microholes film/effusion cooling effectiveness*. J. Therm. Sci. **26**(2017), 5, 459–464.
- [16] SZWABA R., OCHRYMIUK T., LEWANDOWSKI T., CZERWINSKA J.: *Experimental investigation of microscale effects in perforated plate aerodynamics*. J. Fluids Eng. **135**(2013), 12, 121104-1-10